Evaluating Retrofitting Strategies of Low-to-Mid-Rise Reinforced Concrete Structure Based on Its Seismic Fragility

Midia Rahma [a], Senot Sangadji [b,*], Zikra Fauzan Virawan [b], Halwan Alfisa Saifullah [b], Rida Handiana Devi [c]

[a] *Master Program in Civil Engineering, Universitas Sebelas Maret, Surakarta, 57126, Indonesia*
[b] *Department of Civil Engineering, Faculty of Engineering, Universitas Sebelas Maret, Surakarta, 57126, Indonesia*
[c] *Department of Civil Engineering, Faculty of Engineering, Universitas Veteran Bangun Nusantara, Sukoharjo, 57521, Indonesia*
Corresponding author: [*]s.sangadji@ft.uns.ac.id

Abstract— In earthquake-prone regions such as Indonesia, this situation has drawn public attention and led to difficulties in implementing certain policies and decision-making. One of the challenging issues in seismic risk reduction is evaluating the efficacy of seismic retrofitting the existing low-to-mid reinforced concrete building. Therefore, this research evaluates the retrofitting of low-to-mid-rise reinforced concrete structures to evaluate the efficacy of the retrofitting strategy rationally using Fiber Reinforced Plastic (FRP), Buckling Restrained Braced Frame (BRBF), and shear wall strategies. Rusunawa at Cilacap, a mid-rise RC apartment for low-income people, was selected as a benchmark building to compare existing and retrofitted seismic fragility. Furthermore, a 3D computer model was developed to predict the seismic response of the structure using a nonlinear static (pushover) analysis. The pushover method produces a capacity curve, showing that the unreinforced structure has a maximum base shear value of 15.2×10^3 kN. While the reinforcement of low to medium rise reinforced concrete structures using the Fiber Reinforced Plastic strategy has a maximum base shear value of 15.3×10^3 kN, then reinforcement using the Buckling Restrained Braced Frame strategy with a maximum base shear value of 16.2×10^3 kN. The shear wall reinforcement has a value maximum base shear of 19.7×103 kN. The capacity curves as the analysis outputs were then converted into the fragility and used to rationalize the probabilistic value of the damage states between existing and retrofitted buildings.

Keywords— Fragility; retrofitting; nonlinear static (pushover) analysis.

I. INTRODUCTION

Several high seismicity regions worldwide have experienced a significant rise in natural disasters such as earthquakes. In urban areas where development is quite intense, the frequent collapse of some buildings has taken many lives, displaced people from their homes, and disrupted businesses. This huge loss decelerates the regional economic growth of the country at large. In earthquake-prone regions such as Indonesia, this situation has drawn public attention and led to difficulties in implementing certain policies and decision-making. Devising scenarios and related activities, such as disaster prevention and mitigation measures, in the case of earthquakes has become challenging and problematic [1], [2].

Many people have suggested the upgrade of the existing building stock in cities before this event rather than repairing post-earthquake damaged structures. However, decisions regarding the existence of seismic rehabilitation and its cost require comprehensive considerations [3]. It involves both engineering and socio-economic analyses as well as prioritization.

Furthermore, there is a fundamental question concerning ways to devise viable and effective risk reduction plans in engineering. In reality, the question further involves rationally quantifying the risks associated with the selected retrofitting strategy compared to the other designs. Many building stocks are quite vulnerable to earthquake attacks in earthquake areas, as they were designed based on past standards and codes [4]. Therefore, they must be strengthened to improve their capacity, stiffness, and ductility for the rest of their lifetime.

Reinforcement is one of the strategies applied to existing buildings to reduce the risk of structural failure due to earthquakes. In this case, the existing structure was repaired or modified by adding new components to improve seismic

performance. These include a fiber-reinforced polymer (FRP) wrapped on structural elements, buckling restrained brace frame (BRBF), shear wall, seismic isolator, and damper. Seismic retrofitting involving FRP sheet wrapped onto structural frame elements such as columns and beams reinforced by polymer resins acts as external confinement. Its local implementation on structures with potential plastic hinges reduces its lateral deformation, increases its ductility, and enhances the member's capacity to carry the extra load. This, in turn, aids in developing a better global performance of the structure [5]–[7].

Installing concentric brace frames (CBF) or eccentric brace frames (EBF) also improves the seismic resistance of existing buildings and impresses with the simplicity and accuracy of decision-making and construction. Therefore, this metal truss frame was placed in a metal jacket filled with mortar to increase resistance to compressive buckling [8]–[10]. BRBFs resist lateral load as vertical trusses aligned to the axis of the structural frame joints. Shear walls also tend to be installed in the existing structural frame. It is described as a vertical concrete slab constructed on a particular side of the building to enhance its rigidity and bind the largest lateral shear force that occurs due to seismic activities [11]–[13]. However, erecting shear walls in critical locations on the multi-story structure provides the rigidity required for resisting horizontal load economically.

Seismic isolation resists earthquake load by converting its energy into a significant isolator deformation usually placed between the sub- and superstructures. This isolator absorbs enormous kinetic energy from the vibration and displaces the superstructure as a rigid body unshaken by the ground motion [14]–[16]. This research demonstrates how the fragile function of existing structures, retrofitted by FRP, BRBF, and shear walls, is used to evaluate the rational efficacy of the adopted strategy.

II. Materials and Method

The existing building selected for this analysis is Rusunawa Cilacap, a typical mid-rise apartment for low-income people built by the government of the Republic of Indonesia to overcome the growing demand for affordable housing. It is located in Tegal Kamulyan Village, South Cilacap District, Cilacap Regency, situated 1.8 km from Cilacap square. This is the first Rusunawa in Cilacap Regency intended for coastal communities, most of whom are fishermen.

Fig. 1   Rusunawa Cilacap, a typical mid-rise apartment for low-income people

Reinforced concrete (RC) moment resistance frames are at latitude 7.89 and longitude 109.024, and accelerometer response is 0.989 and 0.391 for the short and long term, respectively. Therefore, as shown in Figure 1, it is classified as having reasonably high seismic resistance, including four-story buildings with irregularities and various structural cross-sections floor plans.

The material and the geometric nonlinearity control the 3D computer model representing the structure's global behavior. A discrete 3D FE model was developed in Seismostruct (semisoft), an FE application capable of calculating large deformation and material nonlinearity under static and dynamic loading.

This analysis assigned the distributed inelasticity in the reinforced concrete frame through Fiber Element Modeling (inelastic frame element) [17]. The Navier-Bernoulli approach is used as a delimiter that divides the frame into segments. Figure 1 shows that the sections are discretized into fibers, accurately modeling the nonlinear distribution of the material. Each fiber across the cross-section will be integrated into a stress-strain response. This is done in the selected and integrated sections, Gaussian sections A and B.
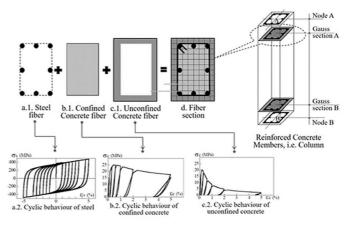

Fig. 2   Fiber element modelling

The periodic stress-strain behavior of the rebar (Figure 2: a.2) was proposed via Menegotto and Pinto and modelled by the equation modified by way of Fillipou to explain the isotropic hardening relation. On the other hand, for non-reinforced concrete, Mander et al. (Figure 2: b.2 and c.2). The existing building was retrofitted in a computer model by adding FRP to the first story's exterior column and installing BRBFs and shear walls in the exterior frames to enhance its seismic performance.

The nonlinear FRP prestressed concrete column was modeled at some point in the FE program based on Ferracuti's work [18]. In addition, the stress-strain relationship is perfectly linear until it breaks [19]. In addition, the FRP layer surrounding the concrete was modeled using the framework proposed by Spoelstra and Monti [20]. CRFP (Carbon Fiber Reinforced Polymer) is installed on the model in two layers of FRP, with a thickness recommendation of 0.17083. The type of CFRP used is SikaWrap600C [21]. Figure 3 shows the building retrofitted with FRP.

BRBF exhibits hysteretic behavior in the core material in tension and compression, leading to large and stable energy dissipation under solid seismic input. A cyclic elastoplastic

constitutive model for steel BRBF was proposed by Zona and Dall'Asta [22]. Figure 4 shows the 3D model of retrofitted buildings developed in Seismostruct.
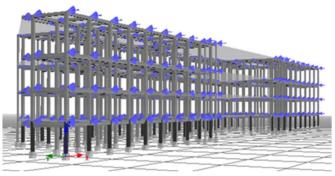

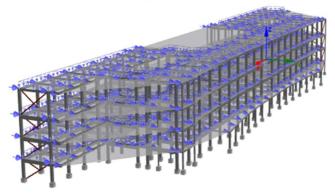Fig. 3 Building retrofitted with FRP

Fig. 4 Building retrofitted with BRBF

Meanwhile, the RC shear wall is a predominant component used in high-rise structures to resist lateral seismic load, and its hysteretic behavior effectively absorbs large seismic energy. Macroscopic models tend to incorporate cyclic softening membranes. In this analysis, the 3D model involving building a retrofit with a shear wall is shown in Figure 5.
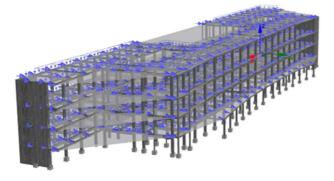

Fig. 5 Building retrofitted with Shearwall

The 3D model will be analyzed using the pushover analysis method. Nonlinear static analysis is a linear and nonlinear two- or three-dimensional static earthquake analysis method, where lateral loads are considered as static loads acting on the center of mass of each floor. The magnitude of the load is increased gradually until it exceeds the load causing yielding at the first plastic hinge in the structure. This condition is continued by increasing the load until it undergoes a large

elastoplastic deformation until the condition is on the verge of collapse [23], [24].

In this analysis, the structure's stiffness is no longer constant by updating each step gradually until a plastic hinge is at the location of the damage to the element. The increase in load will increase deformation when the thrust is applied in the inelastic period. The pushover method produces a capacity curve that plots the basic shear force as a displacement function [25], [26].

Fragility is defined as the probability of damage to the structure that exceeds the demand parameter of a certain level of performance of the structure over its lifetime [27]. This demand parameter reflects seismic intensity, such as peak ground acceleration (PGA), acceleration spectral (Sa), and displacement spectral (Sd).

The fragility function or curve is understood as the 'fingerprint' of a particular building. It reflects the structural response of an individual structure due to external seismic load with the fragility curves developed to predict the structure's potential damage during an earthquake event [28], [29]. These assess seismic risk and indicate the level of physical damage in the strongest seismic main shock [30]. The vulnerability function is defined as the relationship between the intensity earthquake with the possibility of exceeding a certain limit. The conditional probability is formulated as a cumulative distribution function (lognormal) (1) as follows [31].

$$Fragility = P[DS|EDP] \tag{1}$$

Where DS is the damage state (DS) or limit state, EDP is the engineering demand parameter or Intensity measure (IM), such as the ground motion parameter, and y is the realized condition of ground motion. Based on this general relationship, various equations were derived and reported in many studies and used to develop fragility curves.

Analyzing the fragility of existing buildings was initiated by predicting its nonlinear response in silicon-related input (ground motion), structural model (in a computer), and the output, which is the capacity curve. Currently, three types of computer structural models are commonly used, namely (1) Global or collective Parameter Model in which the nonlinear response of a structure is represented with certain degrees of freedom, (2) Discrete Finite Element Model, also known as Structural Element, or Frame Model, where the structural modelling uses a pattern of interconnected truss elements with a nonlinear distribution and (3) Microscopic Finite Element Model.

In developing the fragility curve, the result of the seismostruct output in the form of a capacity curve is converted into a spectra capacity curve and realized without a software analysis in the ADRS (Acceleration Displacement Response Response Response Spectrum) format. Based on ATC-40, the relationship between spectral acceleration and displacement is determined with the following equation.

$$Sa = \frac{V/W}{\alpha 1} \tag{2}$$

$$Sd = \frac{\Delta roof}{PF1.\emptyset roof1} \tag{3}$$

While PF1 and 1 are evaluated with the equation based on FEMA, HAZUZ MH-MR5 is as follows:

$$PF1 = \left[\frac{\sum_{i=l}^{N}(wi.\emptyset i\, l)/g}{\sum_{i=l}^{N}(wi.\emptyset i\, l^2)/g}\right] \qquad (4)$$

$$\alpha 1 = \frac{\left[\sum_{i=l}^{N}(wi.\emptyset i\, l)/g\right]^2}{\left[\sum_{i=l}^{N}(wi)/g\right]\left[\sum_{i=l}^{N}(wi.\emptyset i\, l^2)/g\right]} \qquad (5)$$

Where Sα, Sd, V, W, $\alpha 1$, Δroof, PF1, $\emptyset_i 1$, wi/g as spectral acceleration, spectral displacement, base shear force, structure weight, the modal mass coefficient for the first capital, roof displacement, modal participation for the first capital, the first amplitude for each ith floor, mass on the ith floor.

In the fragility curve formulation, the lognormal standard deviation, β, is expressed as randomness and the uncertainty component of variability. Besides, this shows the probable conditions in relation to Spectral displacement (Sd) based on the damaged state of several methods formulated as follows.

$$P[ds|S_d] = \phi\left[\frac{1}{\beta_{ds}}\ln\left(\frac{S_d}{S_{d,ds}}\right)\right] \qquad (6)$$

Where:

Sd,ds : the median spectral displacement value achieved by the building based on the damaged state

Φ : the standard normal function of the cumulative distribution

The uncertainty in each damage condition can be calculated using the subsequent formulation:

$$(\beta_{ds}) = \sqrt{[(CONV[\beta_c,\beta_d])]^2 + [\beta_{M\,(ds)}]^2} \qquad (7)$$

Source : Hazus-MH MR5

The standard deviation of the structural capability (βc) is calculated using the following equation:

$$\beta c = \sqrt{\ln\left(\frac{s^2}{m^2}+1\right)} \qquad (8)$$

The notations of βc, βd, βM(ds), m, s refer to the standard deviation of the structural capability uncertainty, the standard deviation of the uncertainty of the demand spectrum (where the long and short periods 0.45 and 0.5, respectively, the standard deviation of the uncertainty limit of the damaged condition with a value of 0.4, the mean of the acceleration capability in the controlled structure spectra, the mean of the acceleration capability in the controlled structure spectra, a standard deviation of the accelerating capability in the controlled structure spectra. An easy way to comply with the conference paper formatting requirements is to use this document as a camera-ready template.

III. Results and Discussion

The capacity curve was generated with a nonlinear static procedure that describes the effect of shear forces and roof displacements on the structure when subjected to pushover loads. It was obtained based on the analysis of the seismostruct software program. Figure 6 compares the capacity curves modeled as existing, retrofitted with FRP perimeter, BRBF, and Shear Wall.
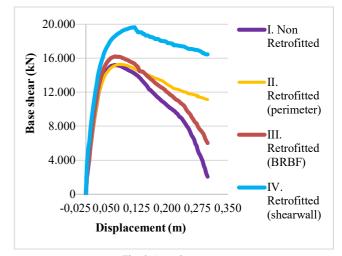

Fig. 6 Capacity curve

The following table summarizes the capacity curves for non-retrofit models, including those with FRP perimeter, BRBF, and Shear Wall at the time of peak shear value for each model.

TABLE I
RECAPITULATION OF BASE SHEAR AT PEAK VALUE

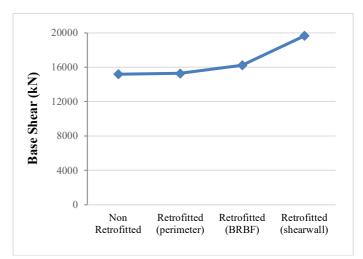|	Displacement	Base Shear	Percentage
Non-Retrofitted	0.069	15190.811	
Retrofitted (Perimeter)	0.084	15279.158	0.578
Retrofitted (BRBF)	0.075	16224.284	6.370
Retrofitted (Shear Wall)	0.120	19661.749	22.739

Fig. 7 Visualization of base shear at peak value

Figure 6 and Table I show that the value of the base shear peak is similar for each model. The decrease in the shear capacity of the non-retrofit model is more significant than the reinforcement structure. In Figure 7, the visualization of the basic shear values for each model is clearly evident. Applying multiple reinforcement strategies increases the maximum base shear value, thereby contributing to the rigidity of the structure.

On the other hand, the maximum base shear value of the structural model with shear walls increases significantly. The structural model without any reinforcement only obtained a basic shear value of 15.2x103 kN. On the other hand, the base shear peak value of the structural model with FRP perimeter reinforcement is 15.3x103 kN, which is larger than that of the unreinforced structural model, with a slight difference. Meanwhile, the structural model with BRBF reinforcement and shear walls increased by 16.2 x 103 kN and 19.7 x 103 kN, respectively. The comparison of the maximum base shear value of the non-retrofit model with the FRP perimeter was increased by 0.5%. On the contrary, the retrofit BRBF experienced an increase of 6.71%, with the highest rise experience by building structures with shear wall retrofit at 29,3% [32].

Two methods, namely HAZUS MH-MR5 and Silva et al [33], were used to determine the effect of damage limitation on the structure's performance. The Hazus MH-MR5 method categorizes the damage limits into slight, moderate, extensive, and complete. The fragility analysis parameters are determined using this method by the displacement spectrum at the damage limit, as shown in Table 2. Based on the Silva et al. [33] method, it is explained that the maximum roof displacement is used to identify the boundary conditions of building damage by being classified into three limit states 1 (LS1), limit state 2 (LS2), and limit state 3 (LS3). The brittleness analysis parameters determined by these two methods are the displacement spectra and the damage limits shown in Table II.

TABLE II
HAZUS MH-MR5 METHOD DAMAGE CRITERIA

Damage Criteria	Retrofitted			
	Non	FRP Perimeter	BRBF	Shear Wall
Slight	0.018	0.019	0.019	0.018
Moderate	0.037	0.037	0.037	0.036
Extensive	0.092	0.093	0.093	0.089
Complete	0.216	0.218	0.216	0.209

TABLE III
METHOD DAMAGE CRITERIA (SILVA ET AL.) [33]

Damage Criteria	Retrofitted							
	Non		FRP Perimeter		BRBF		Shear Wall	
	Sd (m)							
	Δ	Sd	Δ	Sd	Δ	Sd	Δ	Sd
LS1	0.030	0.022	0.027	0.020	0.030	0.022	0.023	0.023
LS2	0.069	0.050	0.084	0.062	0.075	0.055	0.120	0.085
LS3	0.162	0.119	0.231	0.171	0.174	0.174	0.299	0.213

A comparison of the fragility curves shown in Figure 8 illustrates the probabilities of the non-retrofit model, retrofit with FRP perimeter, BRBF, and Shear Wall against performance limitations according to the Hazus MH-MR5 method.

Figure 8 shows that the probability value of the damage is similar for each model from the non-retrofit to those with FRP perimeter, BRBF, and Shear Wall. The difference in probability values is invisible in the fragility curve of each

model because the points are close. The model with FRP perimeter and BRBF shows the damage probability at slight and moderate levels of 100%. On the other hand, there is no decrease in both damage criteria.

Meanwhile, the retrofit with FRP perimeter and BRBF experienced a decrease in the level of extensive and complete damage. The shear wall retrofit on the four damage criteria experienced an increase in probability.
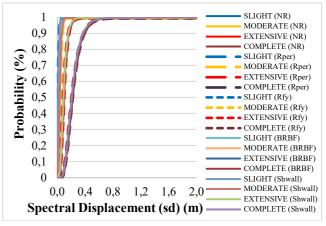

Fig. 8 Fragility curve (Hazus MH-MR5)

A comparison of the fragility curves shown in Figure 9 illustrates the probabilities of the non-retrofit, retrofit with FRP perimeter, BRBF, and Shear Wall against performance limits according to the method proposed by Silva et al. [33].
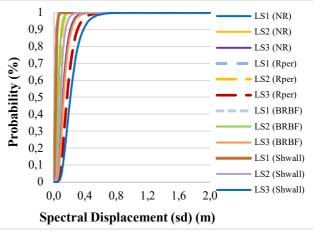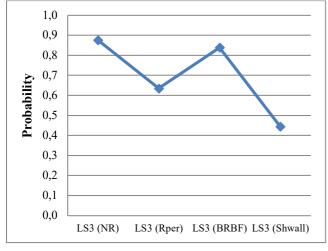

Fig. 9 Fragility curve (Silva et al.) [33]

Table IV is a recapitulation of the probability value of the brittleness curve damage on the LS3 using the Silva et al. [33] method. Meanwhile, the damage probability values for all models are taken at the displacement spectra of 0.2.

TABLE IV
RECAPITULATION OF PROBABILITY VALUES IN LS3

Sd	Damage State	Probabilities	Percentage
0.2	LS3 (NR)	0.875	
	LS3 (RPer)	0.634	-27.532
	LS3 (BRBF)	0.838	-4.241
	LS3 (Swall)	0.445	-49.179

The fragility curve of the Silva et al. [33] method in Figure 9 shows a decrease in the probability value of each model,

including non-retrofits and retrofits with FRP perimeter, BRBF, and Shear Wall. Table 4 shows a decrease in the probability of damage to the models with FRP perimeter, BRBF, and Shear Wall retrofits. The value of these three reinforcements is less than the non-retrofit model at the limit of state 3 (LS3) damage. Figure 10 shows the visualized difference in probability values.

Fig. 10 Visualization of probability values on LS3

IV. CONCLUSION

Buildings with FRP perimeter, BRBF, and Shear Wall retrofits affect their behavior compared to unreinforced. In addition, reinforcement increases the strength and stiffness of the structure. The increase in the base shear value of a building by retrofitted FRP perimeter is 0.5% of the basic value of the non-retrofit building structure. Meanwhile, the structure with BRBF retrofit increased by 6.71%, with the largest increase experienced by the structure with a Shear Wall retrofit of 29.3%. Therefore, its strengthening strategy offers the greatest stiffness contribution.

Fragile curves are used to evaluate the seismic performance of a structure. It shows the conditional probability that a certain level of damage occurs when various ground vibration accelerations are added. Structures with FRP perimeter reinforcement, BRBF, and Shear Wall reduce the probability of exceeding a predetermined limit. Therefore, the fragility curve determines effective reinforcement and reduces the risk of building earthquakes.

REFERENCES

[1] V. Y. Palagala and V. Singhal, "Structural score to quantify the vulnerability for quick seismic assessment of RC framed buildings in India," *Eng. Struct.*, vol. 243, Sep. 2021, doi: 10.1016/J.ENGSTRUCT.2021.112659.

[2] X. Liao, S. Zhang, Z. Cao, and X. Xiao, "Seismic performance of a new type of precast shear walls with non-connected vertical distributed reinforcement," *J. Build. Eng.*, vol. 44, p. 103219, Dec. 2021, doi: 10.1016/J.JOBE.2021.103219.

[3] F. Rezazadeh and S. Talatahari, "Seismic energy-based design of BRB frames using multi-objective vibrating particles system optimization,"

Structures, vol. 24, pp. 227–239, Apr. 2020, doi: 10.1016/J.ISTRUC.2020.01.006.

[4] A. Rahimi and M. R. Maheri, "The effects of steel X-brace retrofitting of RC frames on the seismic performance of frames and their elements," *Eng. Struct.*, vol. 206, no. November 2019, 2020, doi: 10.1016/j.engstruct.2019.110149.

[5] D. A. Pohoryles, J. Melo, T. Rossetto, H. Varum, and L. Bisby, "Seismic Retrofit Schemes with FRP for Deficient RC Beam-Column Joints: State-of-the-Art Review," *J. Compos. Constr.*, vol. 23, no. 4, p. 03119001, 2019, doi: 10.1061/(asce)cc.1943-5614.0000950.

[6] H. H. Mhanna, R. A. Hawileh, and J. A. Abdalla, "Comparative analysis of design guidelines for FRP contribution to shear capacity of strengthened RC beams," *Procedia Struct. Integr.*, vol. 37, pp. 359–366, Jan. 2022, doi: 10.1016/J.PROSTR.2022.01.096.

[7] M. Gotame, C. L. Franklin, M. Blomfors, J. Yang, and K. Lundgren, "Finite element analyses of FRP-strengthened concrete beams with corroded reinforcement," *Eng. Struct.*, vol. 257, p. 114007, Apr. 2022, doi: 10.1016/J.ENGSTRUCT.2022.114007.

[8] S. E. Ruiz *et al.*, "BRB retrofit of mid-rise soft-first-story RC moment-frame buildings with masonry infill in upper stories," *J. Build. Eng.*, vol. 38, p. 101783, 2021, doi: 10.1016/j.jobe.2020.101783.

[9] J. A. Oviedo-Amezquita, N. Jaramillo-Santana, C. A. Blandon-Uribe, and A. M. Bernal-Zuluaga, "Development and validation of an acceptance criteria and damage index for buckling-restrained braces (BRB)," *J. Build. Eng.*, vol. 43, Nov. 2021, doi: 10.1016/J.JOBE.2021.102534.

[10] E. Ballinas, H. Guerrero, A. Terán-Gilmore, and J. Alberto Escobar, "Seismic response comparison of an existing hospital structure rehabilitated with BRBs or conventional braces," *Eng. Struct.*, vol. 243, Sep. 2021, doi: 10.1016/J.ENGSTRUCT.2021.112666.

[11] A. Seifiasl and M. Hoseinzadeh Asl, "Experimental and numerical study on the seismic behavior of steel plate shear wall with reduced web section beams," *J. Build. Eng.*, vol. 46, p. 103797, Apr. 2022, doi: 10.1016/J.JOBE.2021.103797.

[12] F. Wei, H. Chen, and Y. Xie, "Experimental study on seismic behavior of reinforced concrete shear walls with low shear span ratio," *J. Build. Eng.*, vol. 45, p. 103602, Jan. 2022, doi: 10.1016/J.JOBE.2021.103602.

[13] A. M. Abualreesh, A. Tuken, A. Albidah, and N. A. Siddiqui, "Reliability-based optimization of shear walls in RC shear wall-frame buildings subjected to earthquake loading," *Case Stud. Constr. Mater.*, vol. 16, p. e00978, Jun. 2022, doi: 10.1016/J.CSCM.2022.E00978.

[14] J. Zhong, J. Zhang, X. Zhi, and F. Fan, "Probabilistic seismic demand and capacity models and fragility curves for reticulated structures under far-field ground motions," *Thin-Walled Struct.*, vol. 137, pp. 436–447, Apr. 2019, doi: 10.1016/j.tws.2019.01.032.

[15] Y. Peng, Y. Ma, T. Huang, and D. De Domenico, "Reliability-based design optimization of adaptive sliding base isolation system for improving seismic performance of structures," *Reliab. Eng. Syst. Saf.*, vol. 205, p. 107167, 2021, doi: 10.1016/j.ress.2020.107167.

[16] Y. S. Lin, R. W. K. Chan, and H. Tagawa, "Earthquake early warning-enabled smart base isolation system," *Autom. Constr.*, vol. 115, no. December 2019, p. 103203, 2020, doi: 10.1016/j.autcon.2020.103203.

[17] F. F. Taucer, E. Spacone, and F. C. Filippou, "A Fiber Beam-Column Element for Seismic Response Analysis of Reinforced Concrete Structures," *Ucb/Eerc-91/17*, no. December 1991, p. 138, 1991.

[18] B. Ferracuti, M. Savoia, R. Francia, R. Pinho, and S. Antoniou, "Pushover analysis of FRP-retrofitted existing RC frame structures," *FRPRCS-8 Univ. Patras, Patras*, no. June 2014, pp. 1–10, 2007.

[19] R. Pinho, C. Casarotti, and S. Antoniou, "A comparison of single-run pushover analysis techniques for seismic assessment of bridges," *Earthq. Eng. Struct. Dyn.*, vol. 36, no. 10, pp. 1347–1362, 2007, doi: 10.1002/EQE.684.

[20] M. R. Spoelstra and G. Monti, "FRP-Confined Concrete Model," *J. Compos. Constr.*, vol. 3, no. 3, pp. 143–150, Aug. 1999, doi: 10.1061/(ASCE)1090-0268(1999)3:3(143).

[21] R. H. Devi, S. Sangadji, and H. A. Saifullah, "Fragility curve of low-to-mid-rise concrete frame retrofitted with FRP," *E3S Web Conf.*, vol. 156, 2020, doi: 10.1051/e3sconf/202015603006.

[22] A. Zona and A. D. Asta, "Elastoplastic model for steel buckling-restrained braces," *JCSR*, vol. 68, no. 1, pp. 118–125, 2012, doi: 10.1016/j.jcsr.2011.07.017.

[23] W. M. Hassan and J. C. Reyes, "Assessment of modal pushover analysis for mid-rise concrete buildings with and without viscous dampers," *J. Build. Eng.*, vol. 29, p. 101103, May 2020, doi: 10.1016/J.JOBE.2019.101103.

[24] M. Kheirollahi, K. Abedi, and M. R. Chenaghlou, "A new pushover procedure for estimating seismic demand of double-layer barrel vault roof with vertical double-layer walls," *Structures*, vol. 34, pp. 1507–1524, Dec. 2021, doi: 10.1016/J.ISTRUC.2021.08.090.

[25] M. Gholhaki, G. Pachideh, and A. Javahertarash, "Capacity spectrum of SPSW using pushover and energy method without need for calculation of target point," *Structures*, vol. 26, pp. 516–523, Aug. 2020, doi: 10.1016/J.ISTRUC.2020.04.028.

[26] A. Nettis, R. Gentile, D. Raffaele, G. Uva, and C. Galasso, "Cloud Capacity Spectrum Method: Accounting for record-to-record variability in fragility analysis using nonlinear static procedures," *Soil Dyn. Earthq. Eng.*, vol. 150, p. 106829, Nov. 2021, doi: 10.1016/J.SOILDYN.2021.106829.

[27] Y. Liu, J. S. Kuang, Q. Huang, Z. Gu, and X. Wang, "Spectrum-based pushover analysis for the quick seismic demand estimation of reinforced concrete shear walls," *Structures*, vol. 27, no. June, pp. 1490–1500, 2020, doi: 10.1016/j.istruc.2020.07.040.

[28] J. Zhong, J. Zhang, X. Zhi, and F. Fan, "Thin-Walled Structures Probabilistic seismic demand and capacity models and fragility curves for reticulated structures under far- fi eld ground motions," *Thin Walled Struct.*, vol. 137, no. January, pp. 436–447, 2019, doi: 10.1016/j.tws.2019.01.032.

[29] G. Andreotti and C. G. Lai, "Use of fragility curves to assess the seismic vulnerability in the risk analysis of mountain tunnels," *Tunn. Undergr. Sp. Technol.*, vol. 91, p. 103008, Sep. 2019, doi: 10.1016/J.TUST.2019.103008.

[30] M. Bovo and N. Buratti, "Evaluation of the variability contribution due to epistemic uncertainty on constitutive models in the definition of fragility curves of RC frames," *Eng. Struct.*, vol. 188, pp. 700–716, Jun. 2019, doi: 10.1016/J.ENGSTRUCT.2019.03.064.

[31] I. Ratna Hapsari, S. Sangadji, and S. Adi Kristiawan, "Seismic performance of four-storey masonry infilled reinforced concrete frame building," *MATEC Web Conf.*, vol. 195, pp. 1–14, 2018, doi: 10.1051/matecconf/201819502017.

[32] Z. F. Virawan, S. Sangadji, and H. A. Saifullah, "Fragility curves for low-to-mid-rise concrete frame building retrofitted by shear wall-frame system," *IOP Conf. Ser. Earth Environ. Sci.*, vol. 871, no. 1, pp. 0–8, 2021, doi: 10.1088/1755-1315/871/1/012011.

[33] V. Silva, H. Crowley, H. Varum, R. Pinho, and R. Sousa, "Evaluation of analytical methodologies used to derive vulnerability functions," *Earthq. Eng. Struct. Dyn.*, vol. 43, no. 2, pp. 181–204, 2014, doi: 10.1002/EQE.2337.